# $^{155}$Gd Mössbauer study of $GdFe_6Ge_6$



2007 J. Phys.: Condens. Matter 19 216204

(http://iopscience.iop.org/0953-8984/19/21/216204)

J. Phys.: Condens. Matter **19** (2007) 216204 (9pp) doi:10.1088/0953-8984/19/21/216204

# $^{155}$Gd Mössbauer study of $GdFe_6Ge_6$

**J M Cadogan[1,4], D H Ryan[2] and J D Cashion[3]**

[1] School of Physics, The University of New South Wales, Sydney NSW 2052, Australia
[2] Department of Physics and Centre for the Physics of Materials, McGill University, Montreal, QC, H3A 2T8, Canada
[3] School of Physics, Monash University, Clayton, Victoria 3800, Australia

E-mail: J.Cadogan@unsw.edu.au

Received 21 February 2007, in final form 3 April 2007
Published 27 April 2007
Online at stacks.iop.org/JPhysCM/19/216204

**Abstract**

We have studied the magnetic order of the Gd sublattice in $GdFe_6Ge_6$ using the 86.5 keV $^{155}$Gd Mössbauer resonance. The Gd sublattice orders ferromagnetically at 30.8 ± 0.2 K, independently of the Fe sublattice which orders antiferromagnetically at 489 ± 5 K. The $^{155}$Gd hyperfine magnetic field at 5 K is −25.6 ± 0.1 T and the principal component of the electric field gradient tensor ($V_{ZZ}$) is +(5.8 ± 2.1) × $10^{20}$ V m$^{-2}$, which corresponds to a second-order crystal-field lattice coefficient $A_{20}$ of −22 ± 9 K $a_0^{-2}$.

(Some figures in this article are in colour only in the electronic version)

## 1. Introduction

In those $RFe_6Ge_6$ and $RFe_6Sn_6$ (R = rare-earth) intermetallic compounds where the $R^{3+}$ ion has a magnetic moment, the magnetic ordering processes of the R and Fe sublattices are quite independent of one another ([1] and references therein). The Fe sublattice orders antiferromagnetically and its Néel temperature remains essentially constant across a series at ∼485 K for $RFe_6Ge_6$ or ∼555 K for $RFe_6Sn_6$.

For R = Gd–Er, the rare-earth sublattice orders predominantly ferromagnetically, with Curie temperatures ranging from a high of 45 K in $GdFe_6Sn_6$ to 3 K in $ErFe_6Ge_6$.

The magnetic independence of the R and Fe sublattices can be understood by considering the crystal structures of the $RFe_6Ge_6$ and $RFe_6Sn_6$ compounds. These compounds crystallize in either orthorhombic or hexagonal structures which are based on the hexagonal (B35) structure of the parent FeGe or FeSn compounds [2]. The orthorhombic structures are related to the underlying hexagonal cells: *A* (ortho) is parallel to *C* (hex) and *C* (ortho) is parallel to *A* (hex). The $RFe_6Ge_6$ and $RFe_6Sn_6$ compounds are formed by placing R atoms between the hexagonal Fe planes of FeGe or FeSn and the magnetic independence of the R and Fe sublattices is a

[4] Author to whom any correspondence should be addressed.

consequence of the layered structure of these compounds. The binary FeGe magnetic structure consists of ferromagnetic Fe planes coupled antiferromagnetically to each other [3, 4] and the local environment of the R atoms in the $RFe_6Ge_6$ and $RFe_6Sn_6$ compounds leads to a net cancellation of the Fe–R exchange at the R sites, effectively isolating them from the ordering of the Fe moments. The magnetic ordering of the R sublattice, two orders of magnitude lower in temperature than the Fe ordering, is most likely due to an indirect exchange coupling between R moments.

The results of our $^{57}$Fe Mössbauer study of the $RFe_6Ge_6$ series have been reported previously [5]. The hyperfine field at the $^{57}$Fe nuclei is virtually independent of the rare earth present and our low temperature Mössbauer studies show no sign that the magnetic order of the Fe sublattice is affected by the ordering of the R sublattice, in agreement with neutron diffraction work. We have also carried out $^{119}$Sn Mössbauer work on the $RFe_6Sn_6$ series [6–8]. The Sn atoms are non-magnetic but 2/3 of the $^{119}$Sn nuclei experience transferred hyperfine fields of about 24 T from the magnetic Fe sublattice.

In this paper we present the results of our study of $GdFe_6Ge_6$ by $^{155}$Gd Mössbauer spectroscopy in a first attempt to deduce crystal-field parameters which may be relevant in the study of the variety of R-sublattice magnetic structures found in the $RFe_6Ge_6$ and $RFe_6Sn_6$ compounds.

## 2. Experimental methods

The $GdFe_6Ge_6$ sample was prepared by arc-melting stoichiometric amounts of the pure elements (Gd: 99.9%, Fe: 99.95%, Ge: 99.999%) under Ti-gettered argon. The sample was subsequently annealed at 900 °C for two weeks, sealed under vacuum in a quartz tube.

Sample quality was verified by powder x-ray diffraction with Cu K$\alpha$ radiation on an automated Nicolet-Stoe diffractometer. The diffraction pattern was refined using the Rietveld method and the FULLPROF/WinPLOTR program [9]. The Néel temperature of the Fe sublattice in $GdFe_6Ge_6$ was measured by differential scanning calorimetry on a Perkin-Elmer DSC-7, using the heat capacity peak at $T_N$ as the signature of magnetic ordering. The ordering temperature of the Gd sublattice was determined by ac-susceptibility measurements made on a LakeShore 7100 closed-cycle susceptometer with an ac magnetic field of 700 A m$^{-1}$ (rms) and a frequency of 137 Hz. Magnetization measurements were made on a Quantum Design PPMS.

$^{155}$Gd Mössbauer spectroscopy was carried out at 5 K in transmission mode with a neutron-irradiated $^{154}SmPd_3$ source, also maintained at 5 K. The 86.5 keV gamma-rays were detected using a HPGe detector. The spectrum was least-squares fitted by diagonalization of the full nuclear hyperfine Hamiltonian, using the transmission integral method.

## 3. Results and discussion

### *3.1. Structural, magnetic and hyperfine results*

The annealed sample of $GdFe_6Ge_6$ was virtually single phase, with traces of $Gd_2O_3$ and $Gd_5Ge_4$ present in the total amount of 4 wt%, as determined from the refinement of the x-ray diffraction pattern.

$GdFe_6Ge_6$ forms in the hexagonal $YCo_6Ge_6$-type structure with the $P6/mmm$ (#191) space group. The lattice parameters (at 295 K) are $a = 5.122 \pm 0.003$ Å and $c = 4.071 \pm 0.003$ Å. The crystal structure of $GdFe_6Ge_6$ is shown in figure 1 and the crystallographic data for the Gd, Fe and Ge sites are given in table 1. The x-ray powder diffraction pattern of $GdFe_6Ge_6$ is shown in figure 2.

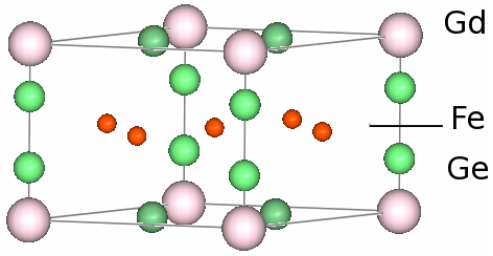


**Figure 1.** Crystal structure of $GdFe_6Ge_6$. The crystal $C$-axis is vertical. (Drawn using the FULLPROF-Studio program [9].)

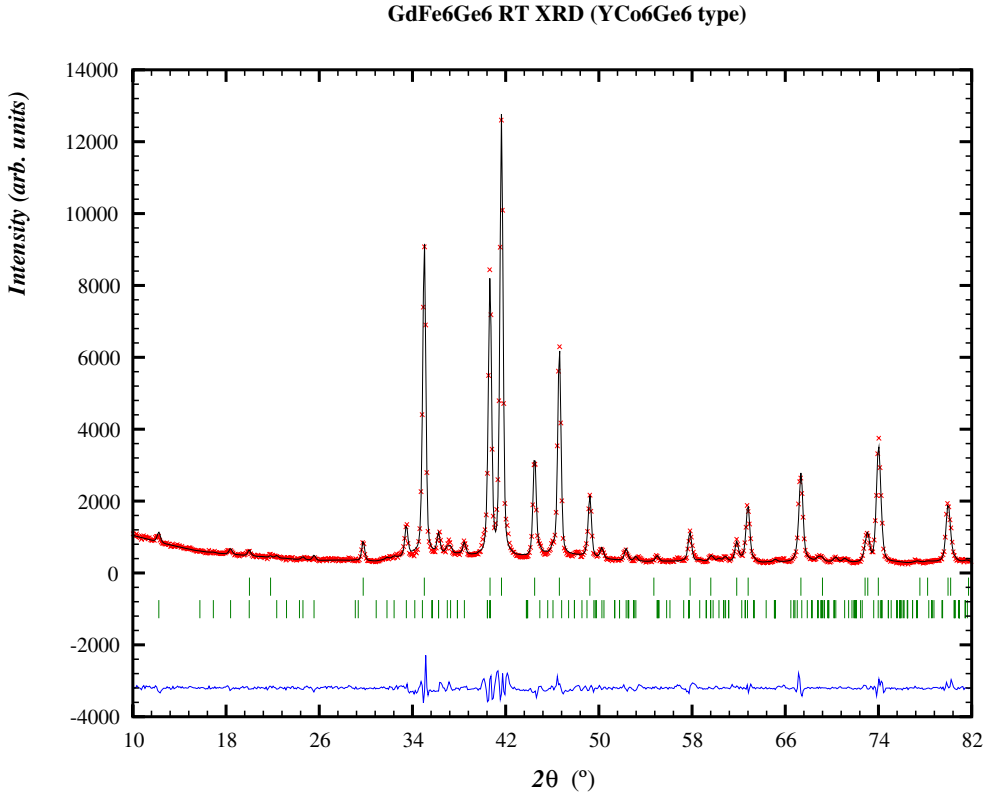


**Figure 2.** X-ray powder diffraction pattern of $GdFe_6Ge_6$, obtained at room temperature with Cu K$\alpha$ radiation. The upper set of Bragg markers refers to the principal $GdFe_6Ge_6$ phase while the lower set refers to the minor impurity phases (see text).

The Néel temperature of the Fe sublattice is 489 $\pm$ 5 K and the Curie temperature of the Gd sublattice is 30.8 $\pm$ 0.2 K. The magnetization of $GdFe_6Ge_6$ amounts to 5.5 $\pm$ 0.5 $\mu_B$/Gd at 2 K, somewhat lower than the $Gd^{3+}$ 'free-ion' value of 7.0 $\mu_B$. This suggests that the magnetic ordering of the Gd sublattice is not perfectly ferromagnetic but includes an antiferromagnetic component, resulting in a canted structure, as found with other R elements.

In figure 3 we show the ac-susceptibility of $GdFe_6Ge_6$. The characteristic 'ferromagnetic' ordering of the Gd sublattice at 30.8 $\pm$ 0.2 K is clear.

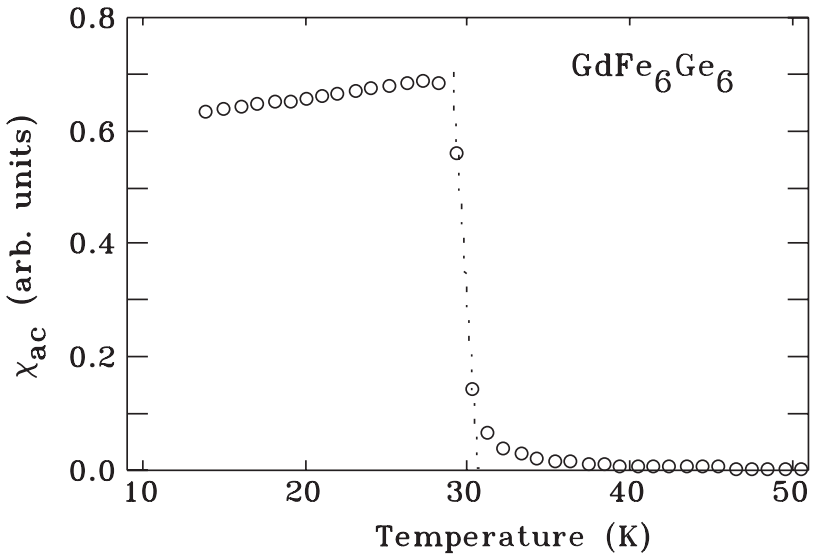


**Figure 3.** The ac susceptibility of $GdFe_6Ge_6$.

**Table 1.** Crystallographic data for $GdFe_6Ge_6$.

| Atom | Site | Point symmetry | $x$ | $y$ | $z$ | Occupancy |
|---|---|---|---|---|---|---|
| Gd | 1a | $6/mmm$ | 0 | 0 | 0 | 0.5 |
| Fe | 3g | $mmm$ | $\frac{1}{2}$ | 0 | $\frac{1}{2}$ | 1.0 |
| Ge | 2c | $\bar{6}m2$ | $\frac{1}{3}$ | $\frac{2}{3}$ | 0 | 1.0 |
| Ge | 2e | $6mm$ | 0 | 0 | 0.30(1) | 0.5 |

In figure 4 we show the $^{155}$Gd Mössbauer spectrum of $GdFe_6Ge_6$, obtained at 5 K. The magnitude of the hyperfine field ($B_{hf}$) at the $^{155}$Gd nucleus is 25.6 $\pm$ 0.1 T. The electric quadrupole interaction at the Gd nuclei is quite simple due to the $6/mmm$ point symmetry of the Gd site in $GdFe_6Ge_6$ which yields an electric field gradient (EFG) asymmetry parameter $\eta = 0$. The principal ($Z$) axis of the EFG tensor is along the hexagonal $C$-axis. The Mössbauer, NMR/NQR and neutron work cited in this paper (*vide infra*) indicates that the $Gd^{3+}$ 4f electronic moment is aligned in the hexagonal plane and therefore the angle $\theta$ between $B_{hf}$ and the EFG $Z$-axis is $\theta = 90°$.

In the absence of an externally applied magnetic field we cannot directly determine the sign of the $^{155}$Gd hyperfine field. Furthermore, we can only determine the sign of the electric quadrupole coupling constant $eQV_{ZZ}$ relative to that of $B_{hf}$. However, as we argue below, $B_{hf}$ is almost certainly negative, the negative sign indicating that $B_{hf}$ is antiparallel to the $Gd^{3+}$ 4f electronic moment. The fitted ground state quadrupole coupling constant at 5 K is $eQV_{ZZ} = -0.261 \pm 0.089$ mm s$^{-1}$: we stress that the negative sign here simply indicates that $eQV_{ZZ}$ has the opposite sign to $B_{hf}$. The isomer shift is $+0.482 \pm 0.004$ mm s$^{-1}$, relative to the $SmPd_3$ source. (For the benefit of the reader we note that 1 mm s$^{-1}$ converts to $4.625 \times 10^{-26}$ J for the 86.5 keV Mössbauer transition in $^{155}$Gd.)

Thus, with $B_{hf}$ negative, our fit to the $^{155}$Gd spectrum of $GdFe_6Ge_6$ yields an electric quadrupole coupling constant (ground state) of $eQV_{ZZ} = +(0.261 \pm 0.089)$ mm s$^{-1}$. The corresponding value of the principal component of the EFG tensor is

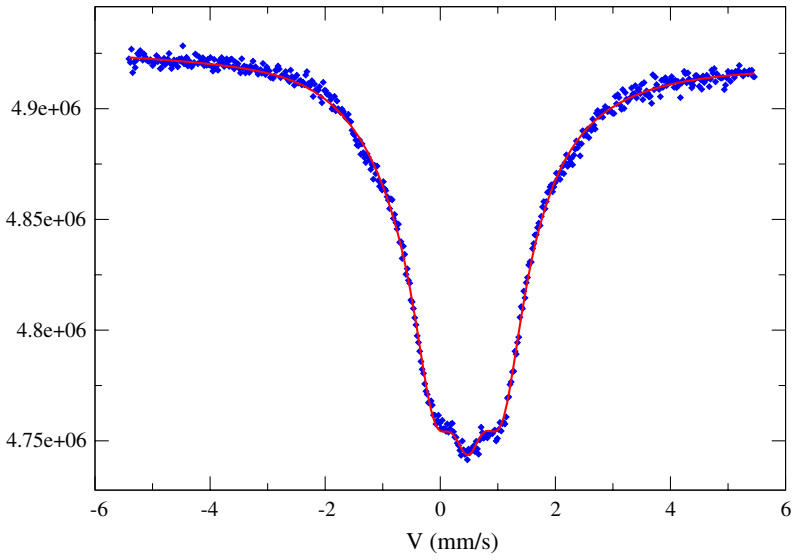


**Figure 4.** $^{155}$Gd Mössbauer spectrum of $GdFe_6Ge_6$ obtained at 5 K.

**Table 2.** Magnetic hyperfine fields (in teslas) at the $^{155}$Gd nuclei in various Gd intermetallics at $T \approx 4$ K.

| Compound | $B_{hf}$ (T) | Reference |
|---|---|---|
| $GdFe_6Ge_6$ | $-25.6 \pm 0.1$ | This work |
| $GdCr_6Ge_6$ | $-26.4 \pm 0.5$ | [11] |
| $GdMn_6Ge_6$ | $-7.4 \pm 0.5$ | [12] |
| $GdMn_6Ge_6$ | $\pm 7.51$ | [19] |
| $GdMn_6Sn_6$ | $\pm 11.6 \pm 0.9$ | [17] |
| $GdMn_6Sn_6$ | $-4.0 \pm 0.5$ | [18] |
| $TbMn_6Sn_6$ (n.b. $^{159}$Tb) | $24.0 \pm 0.1$ | [22] |
| $GdT_2Si_2$ | $-24.6$ to $-32.7$ | [16] |
| T = Cr, Mn, Fe, Co, Ni, Cu, Ru, Rh, Pd, Ag, Os, Ir, Au | | |

$V_{ZZ} = +(5.8 \pm 2.1) \times 10^{20}$ V m$^{-2}$, using a value of $+1.30 \pm 0.02$ *b* for the $^{155}$Gd ground state quadrupole moment [10].

### *3.2. Magnetic hyperfine field*

In this section we shall put our magnetic hyperfine field determination into context, with reference to a variety of Gd-based intermetallic compounds. For the convenience of the reader we present in table 2 a summary of the hyperfine field data germane to the following analysis.

Our measured hyperfine field value of $-25.6 \pm 0.1$ T is consistent with the value of $-26.4 \pm 0.5$ T in $GdCr_6Ge_6$ reported by Mulder *et al* [11]. The Cr sublattice in $GdCr_6Ge_6$ was shown to be non-magnetic by neutron diffraction [13].

The hyperfine magnetic field at the $^{155}$Gd nucleus in $GdFe_6Ge_6$ can be written as

$$B_{hf} = B_{4f} + B_{cp} + B_p + B_{nn}^{Gd} + B_{nn}^{Fe} + B_{ext} \quad (1)$$

where

- $B_{4f}$ is the field due to the incomplete 4f electron shell.

- $B_{cp}$ is the core polarization field arising from the deformations of the inner electronic shells by the $Gd^{3+}$ 4f shell.
- $B_p$ is the contribution from conduction electron polarization by the spin of the parent $Gd^{3+}$ ion.
- $B_{nn}^{Gd}$ and $B_{nn}^{Fe}$ are transferred hyperfine fields from the surrounding magnetic Gd and Fe sublattices, respectively, mediated by conduction electron polarization.
- $B_{ext}$ represents an externally applied magnetic field.

The intra-ionic 'free-ion' field is the sum of $B_{4f}$ and $B_{cp}$ for the unquenched electronic state $|\langle J_z\rangle| = J$ and amounts to $-32.2$ T for $Gd^{3+}$, i.e. antiparallel to the parent $Gd^{3+}$ 4f magnetic moment [14, 15]. The transferred hyperfine field $B_{nn}^{Fe}$ is zero since the Fe magnetic order is antiferromagnetic and the Fe nearest neighbours of a Gd nucleus are arranged in two ferromagnetic planes, coupled antiparallel to each other. Finally, we have no externally applied magnetic field. Thus, the hyperfine magnetic field (in teslas) at the $^{155}$Gd nucleus is

$$B_{hf} = -32.2 + B_p + B_{nn}^{Gd}. \tag{2}$$

The implicit assumption that the $Gd^{3+}$ moment is completely unquenched is justified because $Gd^{3+}$ is an S-state ion.

Our measured hyperfine field $(\pm)25.6 \pm 0.1$ T yields possible values for $B_p + B_{nn}^{Gd}$ of 6.6 T ($-$ sign) or 57.8 T ($+$ sign); the latter figure seems improbably large, given that the Gd atom in $GdFe_6Ge_6$ has no Gd nearest neighbours in its first coordination shell. In fact, in our recent $^{166}$Er Mössbauer study of $ErFe_6Sn_6$, we estimated $B_{nn}^{Er}$ at only 0.7 T [8].

We may estimate the self-polarization field $B_p$ by considering the $^{155}$Gd Mössbauer data on 13 $GdT_2Si_2$ (T = transition metal) intermetallic compounds reported by Dirken *et al* [16]. The observed $^{155}$Gd hyperfine fields span a range of $-24.6$ to $-32.7$ T, with an average of $-28.4$ T, omitting the value for $GdMn_2Si_2$ in which the transition metal sublattice is magnetic. Furthermore, the Gd magnetic order is antiferromagnetic. Therefore, there are no transferred fields at the $^{155}$Gd nucleus and the difference between the measured field and the intra-ionic free-ion field ($-32.2$ T) represents $B_p$. Thus, $B_p$ is in the range of $-0.5$ to $+7.6$ T, with the average field corresponding to $B_p = 3.8$ T.

The greatly reduced $^{155}$Gd hyperfine fields in $GdMn_6Sn_6$ ($11.6 \pm 0.9$ T [17], $-4.0 \pm 0.5$ T [18]), and $GdMn_6Ge_6$ ($-7.4 \pm 0.5$ T [12, 19–21]) illustrate the effect of the transferred field from the Mn sublattice. Taking our $^{155}GdFe_6Ge_6$ field of $-25.6 \pm 0.1$ T together with the $GdCr_6Ge_6$ field of $-26.4 \pm 0.5$ T [11], we deduce transferred hyperfine fields from the Mn sublattice of $+22.0 \pm 0.8$ T in $GdMn_6Sn_6$ and $+18.5 \pm 0.4$ T in $GdMn_6Ge_6$ (although we note here that the magnetic structure of the latter is actually a planar spiral, rather than a 'simple' collinear ferrimagnet).

These values of the transferred hyperfine field at the $^{155}$Gd nucleus in $GdMn_6X_6$ (X = Ge, Sn) compare well with the value of $\sim+24$ T deduced by Li *et al* [22] from their $^{159}$ Tb NMR study of $TbMn_6Sn_6$ and $TbMn_6Ge_6$. The $TbMn_6Sn_6$ value translates to $\sim+23.5$ T acting on $^{155}$Gd when we scale with the respective s-electron hyperfine coupling parameters for Tb and Gd, deduced by linear interpolation of the values for $La^{3+}$ and $Lu^{3+}$, given by Campbell [23].

Thus, we may safely conclude that the hyperfine magnetic field at the $^{155}$Gd nucleus in $GdFe_6Ge_6$ is negative i.e. $B_{hf}$ is directed antiparallel to the $Gd^{3+}$ 4f electronic moment.

### *3.3. Electric quadrupole interaction*

As in the preceding section, we shall put our determination of the $^{155}$Gd EFG in $GdFe_6Ge_6$ into context, with reference to a variety of Gd-based intermetallic compounds and for the convenience of the reader we present in table 3 a summary of the EFG data pertaining to our analysis.

**Table 3.** Principal EFG component ($V_{ZZ}$) (in units of $10^{21}$ V m$^{-2}$) at the $^{155}$Gd nuclei in various Gd intermetallics at $T \approx 4$ K. The signs in parantheses were obtained under the assumption that the hyperfine fields were positive.

| Compound | $V_{ZZ}$ | Reference |
|---|---|---|
| $GdFe_6Ge_6$ | $+0.58 \pm 0.21$ | This work |
| $GdCr_6Ge_6$ | $(-)2.9 \pm 0.3$ | [11] |
| $GdMn_6Ge_6$ | $(-)3.4 \pm 0.3$ | [12] |
| $GdMn_6Sn_6$ | $(-)2.0 \pm 0.3$ | [17] |
| $GdMn_6Sn_6$ | $1.98 \pm 0.07$ | [18] |

The EFG at the rare-earth nuclei in intermetallic compounds generally contains contributions from the 4f and valence electronic shells of the parent $R^{3+}$ ion and the surrounding lattice charges (including conduction electrons). $Gd^{3+}$ is an S-state ion and thus the 4f contribution to the EFG is zero. The contribution from the asphericity of the $Gd^{3+}$ 6p and 5d valence electron charge density most likely dominates the contribution of the lattice, as shown by Coehoorn *et al* [24]. This is an important point as it suggests that the so-called 'lattice EFG' is in fact more a *local* property. Thus, the usual assumption of direct proportionality between the *non*-4f EFG and the second-order crystal-field lattice summation terms, in particular the assumption that $A_{20} \propto V_{ZZ}$, using standard notation, lacks a physical basis. However, this is nonetheless a useful approximation and for the purposes of this paper, we will continue with this approximation.

Malaman *et al* [18] have used short-wavelength (0.499 Å) neutron diffraction to show that the Gd and Mn moments in $GdMn_6Sn_6$ are ferrimagnetically coupled in the hexagonal plane i.e. perpendicular to the crystal $C$-axis, which is the $Z$-axis of the $^{155}$Gd EFG. Their measured electric quadrupole coupling constant $eQV_{ZZ}$ of 0.89 mm s$^{-1}$ leads to $V_{ZZ} = \pm (1.98 \pm 0.07) \times 10^{21}$ V m$^{-2}$. Mulder *et al* [11] deduced $V_{ZZ} = -(2.9 \pm 0.3) \times 10^{21}$ V m$^{-2}$ for $GdCr_6Ge_6$ and $V_{ZZ} = -(3.4 \pm 0.3) \times 10^{21}$ V m$^{-2}$ for $GdMn_6Ge_6$. However, we consider the signs of the latter two results to be incorrect since these authors did not deduce the sign of the hyperfine field and one can only measure the relative sign between $eQV_{ZZ}$ and $B_{hf}$, as discussed earlier. The reported signs merely reflect the value of the standard angular term $\frac{1}{2}(3\cos^2\theta - 1)$ employed when rotating the EFG frame onto that defined by the direction of $B_{hf}$, (e.g. [25]).

In deriving the second-order crystal-field term $A_{20}$ from $V_{ZZ}$ one often writes:

$$A_{20} = -\frac{e}{4} V_{ZZ} \Big/ \left( \frac{1 - \gamma_\infty}{1 - \sigma_2} \right) \tag{3}$$

where $\gamma_\infty$ is the Sternheimer antishielding factor and $\sigma_2$ is the lattice shielding factor.

As stated above, we will simply assume that linear proportionality holds i.e.

$$A_{20} = -\frac{e}{4} V_{ZZ}/C \tag{4}$$

and we will use available data on the well-researched $R_2Fe_{14}B$ series to deduce a reasonable value for the proportionality factor ($C$) between $A_{20}$ and $V_{ZZ}$, which we believe will be generally applicable to rare-earth–Fe-rich intermetallics. Bogé *et al* [26] carried out a comprehensive $^{155}$Gd Mössbauer study of $Gd_2Fe_{14}B$, using both powder and single-crystal samples, with and without an externally applied magnetic field, and obtained a value of $-3.50 \pm 0.14$ mm s$^{-1}$ for $eQV_{ZZ}$ at the Gd 4f-site in this tetragonal structure. We will concentrate on the 4f-site since the $Z$ (EFG) and the $Gd^{3+}$ moment are both along the tetragonal $C$-axis at this site. The other Gd site (4g) in $Gd_2Fe_{14}B$ has its $Z$ (EFG) axis perpendicular to the

$Gd^{3+}$ moment. The point symmetries of the two Gd sites in $Gd_2Fe_{14}B$ are both orthorhombic *mm* so each will have a non-zero EFG asymmetry parameter $\eta$. These parameters were also deduced by Bogé *et al* [26] and they have been included in the following analysis.

The measured $eQV_{ZZ}$ at the Gd 4f site in $Gd_2Fe_{14}B$ yields $V_{ZZ} = -(7.77 \pm 0.30) \times 10^{21}$ V m$^{-2}$. The lattice crystal-field coefficients in the $R_2Fe_{14}B$ series were determined by Givord *et al* [27] using single-crystal magnetization data. They found an average $A_{20}$ value of 298 $\pm$ 6 K $a_0^{-2}$ (=1.47 $\pm$ 0.03 J m$^{-2}$) across the $R_2Fe_{14}B$ series; ($a_0$ is the Bohr radius). Thus, the dimensionless proportionality constant between $A_{20}$ (in J m$^{-2}$) and $V_{ZZ}$ (in V m$^{-2}$) is $C = 212 \pm 9$. Our measured $eQV_{ZZ}$ value of $+0.261 \pm 0.089$ mm s$^{-1}$ yields $V_{ZZ} = +(5.8 \pm 2.1) \times 10^{20}$ V m$^{-2}$, which therefore converts to a second-order crystal-field lattice coefficient of $A_{20} = -0.109 \pm 0.045$ J m$^{-2}$ $= -22 \pm 9$ K $a_0^{-2}$.

The above scaling can be re-expressed as simple multiplicative factors of either (i) $-85 \pm 5$ to convert $eQV_{ZZ}$, in units of mm s$^{-1}$, to $A_{20}$ in units of K $a_0^{-2}$, or (ii) $-38 \pm 2$ to convert $V_{ZZ}$, in units of $10^{21}$ V m$^{-2}$, to $A_{20}$ in units of K $a_0^{-2}$. We note that in a summary of numerous $^{155}$Gd Mössbauer studies of a variety of Gd intermetallics Buschow *et al* [28] deduced a range of $-32$ to $-46$ for this latter scaling factor.

To check the sign of our deduced crystal-field term $A_{20}$, we may consider the compounds $ErFe_6Ge_6$ [29] and $DyFe_6Ge_6$ [30]. The second-order Stevens coefficient $\alpha_J$, which facilitates the conversion of the crystal-field lattice summation $A_{20}$ into the $R^{3+}$—specific crystal-field parameter $B_{20}$, is positive for $Er^{3+}$ and negative for $Dy^{3+}$. Therefore, $B_{20}$ is negative for $Er^{3+}$ and positive for $Dy^{3+}$ and assuming that the $R^{3+}$ ordering direction is primarily dictated by the second-order crystal field we would expect the Er sublattice in $ErFe_6Ge_6$ to order parallel to the hexagonal $C$-axis whereas the Dy sublattice in $DyFe_6Ge_6$ would be expected to order perpendicular to the hexagonal $C$-axis. Both $ErFe_6Ge_6$ and $DyFe_6Ge_6$ are orthorhombic and the R ordering directions are $A$ and $C$, respectively, referred to the orthorhombic cell. This cell is derived from the hexagonal $P6/mmm$ B35 cell, as discussed earlier, where we saw that $A$ (ortho) is parallel to $C$ (hex) and $C$ (ortho) is parallel to $A$ (hex). Therefore, the observed ordering directions in $ErFe_6Ge_6$ and $DyFe_6Ge_6$ are fully consistent with our derived value of $A_{20}$.

## 4. Conclusions

We have studied the magnetic ordering of the Gd sublattice in $GdFe_6Ge_6$ by $^{155}$Gd Mössbauer spectroscopy. The Gd sublattice orders at 30.8 $\pm$ 0.2 K. The $^{155}$Gd hyperfine field at 5 K is $-25.6 \pm 0.1$ T and the principal component of the EFG tensor is $V_{ZZ} = +(5.8 \pm 2.1) \times 10^{20}$ V m$^{-2}$, which converts to a crystal-field lattice coefficient of $A_{20} = -22 \pm 9$ K $a_0^{-2}$.

## Acknowledgments

This work was supported by grants from the Australian Research Council, the Natural Sciences and Engineering Research Council of Canada and Fonds pour la formation de chercheurs et l'aide à la recherche, Québec. We are grateful to C Voyer (McGill) for the x-ray diffraction pattern.

## References

[1] Cadogan J M and Ryan D H 2001 *J. Alloys Compounds* **326** 166–73
[2] Chafik El Idrissi B, Venturini G and Malaman B 1991 *Mater. Res. Bull.* **26** 1331–8
[3] Beckman O, Carrander K, Lundgren L and Richardson M 1972 *Phys. Scr.* **6** 151–7

[4] Häggström L, Ericsson T, Wäppling R and Chandra K 1975 *Phys. Scr.* **11** 47–54
[5] Ryan D H and Cadogan J M 1996 *J. Appl. Phys.* **79** 6004–6
[6] Cadogan J M, Suharyana, Ryan D H, Moze O and Kockelmann W 2000 *J. Appl. Phys.* **87** 6046–8
[7] Cadogan J M, Suharyana, Ryan D H, Moze O and Kockelmann W 2001 *IEEE Trans. Magn.* **37** 2606–8
[8] Cadogan J M, Ryan D H, Moze O, Suharyana and Hofmann M 2003 *J. Phys.: Condens. Matter* **15** 1757–71
[9] Rodríguez-Carvajal J 1993 *Physica* B **192** 55–69
Roisnel T and Rodríguez-Carvajal J 2001 *Mater. Sci. Forum* **378–381** 118–23
Chapon L and Rodríguez-Carvajal J 2004 *FULLPROF-Studio* part of the FULLPROF/WinPLOTR suite
[10] Tanaka Y, Laubacher D B, Steffen R M, Shera E B, Wohlfahrt H D and Hoehn M V 1982 *Phys. Lett.* B **108** 8–10
[11] Mulder F M, Thiel R C, Brabers J H V J, de Boer F R and Buschow K H J 1993 *J. Alloys Compounds* **198** L1–3
[12] Mulder F M, Thiel R C, Brabers J H V J, de Boer F R and Buschow K H J 1993 *J. Alloys Compounds* **190** L29–31
[13] Schobinger-Papamantellos P, Rodríguez-Carvajal J and Buschow K H J 1997 *J. Alloys Compounds* **256** 92–6
[14] Bleaney B 1979 *Magnetic Properties of Rare Earth Metals* ed R J Elliott (New York: Plenum) chapter 8
[15] Bleaney B 1988 *Handbook on the Physics and Chemistry of Rare Earths* vol 11, ed K A Gschneidner Jr and L Eyring (Amsterdam: Elsevier) chapter 77
[16] Dirken M W, Thiel R C and Buschow K H J 1989 *J. Less-Common Met.* **147** 97–104
[17] Dirken M W, Thiel R C, Brabers J H V J, de Boer F R and Buschow K H J 1991 *J. Alloys Compounds* **177** L11–5
[18] Malaman B, Venturini G, Welter R, Sanchez J P, Vulliet P and Ressouche E 1999 *J. Magn. Magn. Mater.* **202** 519–34
[19] Kelemen M T, Rösch P, Kaplan N and Dormann E 2000 *Eur. Phys. J.* B **18** 435–40
[20] Kelemen M T, Rösch P, Dormann E and Buschow K H J 2001 *J. Magn. Magn. Mater.* **223** 253–60
[21] Rösch P, Kelemen M T, Dormann E, Tomka G and Riedi P C 2000 *J. Phys.: Condens. Matter* **12** 1065–84
[22] Li Y, Graham R G, Bunbury D St P, Mitchell P W, McCausland M A H, Chaughule R S, Gupta L C, Vijayaraghavan R and Godart C 1995 *J. Magn. Magn. Mater.* **140–144** 1031–2
[23] Campbell I A 1969 *J. Phys. C: Solid State Phys.* **2** 1338–51
[24] Coehoorn R, Buschow K H J, Dirken M W and Thiel R C 1990 *Phys. Rev.* B **42** 4645–55
[25] Cadogan J M and Ryan D H 2004 *Hyperfine Interact.* **153** 25–41
[26] Bogé M, Czjzek G, Givord D, Jeandey C, Li H S and Oddou J L 1986 *J. Phys. F: Met. Phys.* **16** L67–72
[27] Givord D, Li H S, Cadogan J M, Coey J M D, Gavigan J P, Yamada O, Maruyama H, Sagawa M and Hirosawa S 1988 *J. Appl. Phys.* **63** 3713–6
[28] Buschow K H J, Mulder F M and Thiel R C 1998 *J. Alloys Compounds* **275–277** 498–504
[29] Oleksyn O, Schobinger-Papamantellos P, Rodríguez-Carvajal J, Brück E and Buschow K H J 1998 *J. Alloys Compounds* **257** 36–45
[30] Cadogan J M, Ryan D H and Swainson I P 2000 *J. Phys.: Condens. Matter* **12** 8963–71